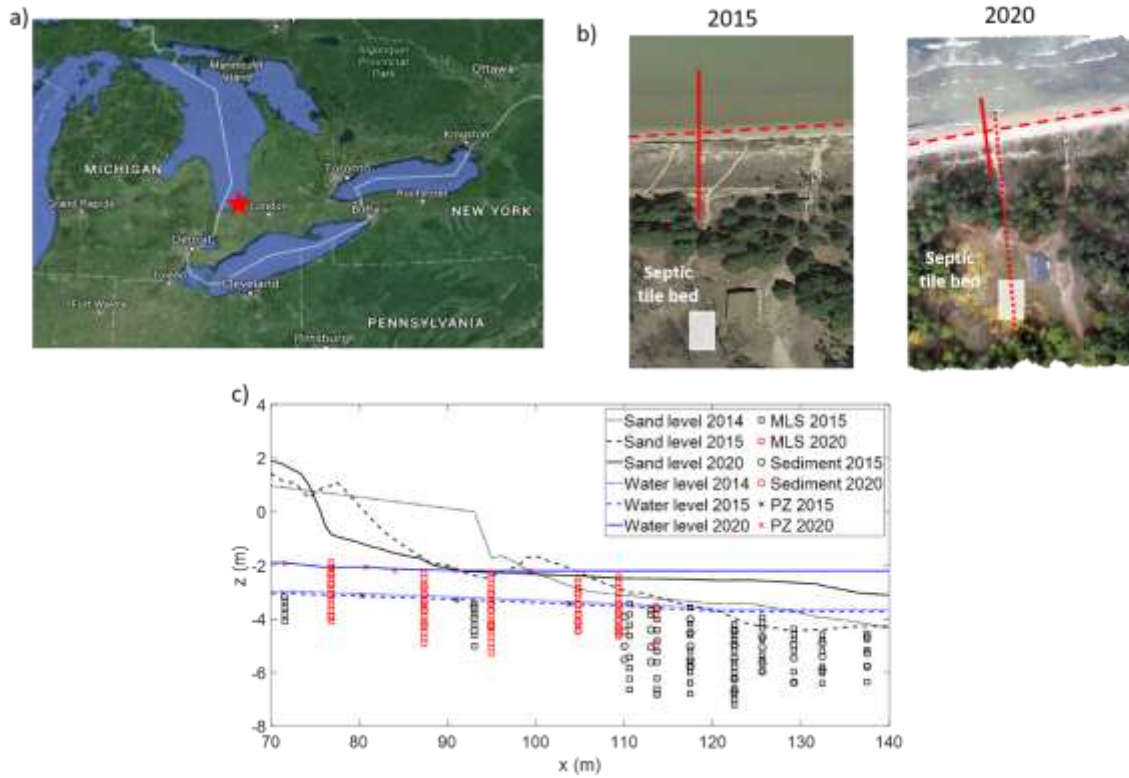
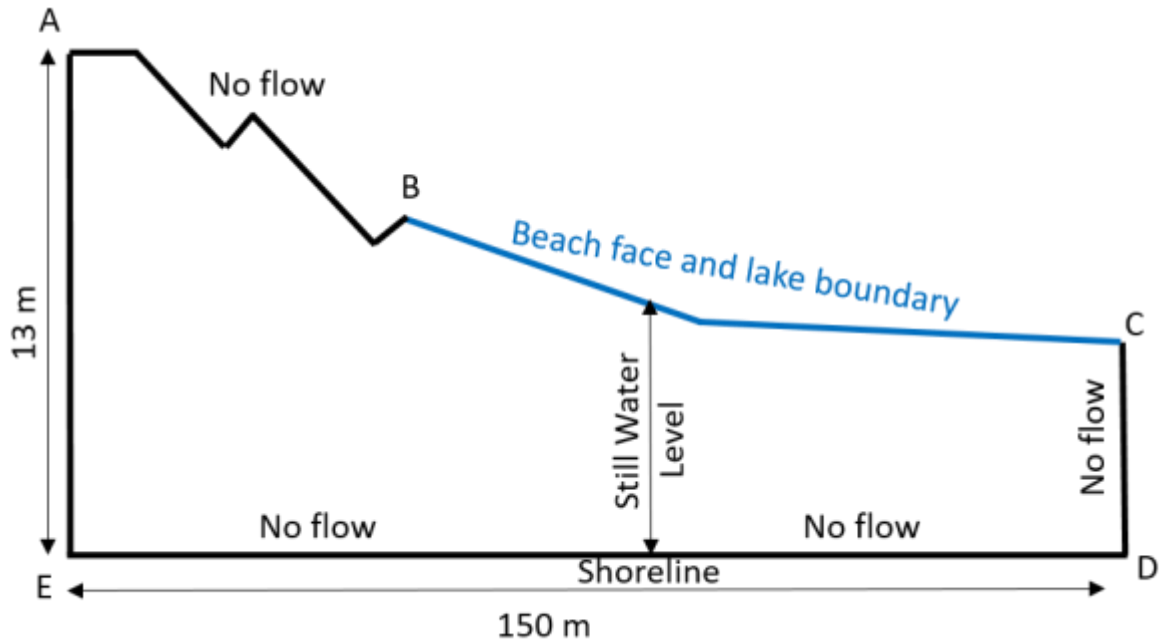


Abstract Art



**Figure 1.** a) Map of Laurentian Great Lakes Basin with the red star indicating the location of the study site. b) Aerial image of the study site using Google Earth imagery in 2015 and Drone (DJI Mavic Air) image in 2020, red dashed lines indicate the shoreline location in each image, solid red lines indicate the cross-shore monitoring transect location, and red dotted line indicates the ERT survey line. The location of septic tile bed is marked with a white rectangle. c) Layout of monitoring equipment along the cross-shore transect for sampling events in 2014 and 2015, and in 2020. Sand and water levels measured in 2014, 2015 and 2020 are also shown in (c).



**Figure 2.** Numerical groundwater model domain including flow boundary conditions.

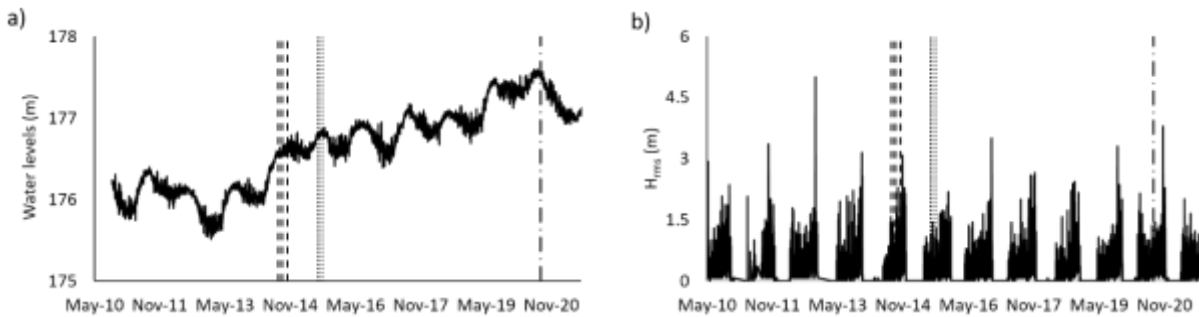


**Figure 3.** a) Average daily lake water levels measured at offshore buoy located 70 km north of the study site (Lake Huron at Goderich (02FE012) with elevation based on International Great Lakes Datum 1985 (Fisheries and Oceans Canada, 2020). b) Offshore root mean square wave height ( $H_{rms}$ ) measured at a buoy (C45149 Southern Lake H) located ~35 km offshore from the field site. The vertical black dashed lines in a) and b) indicate days of field sampling events.

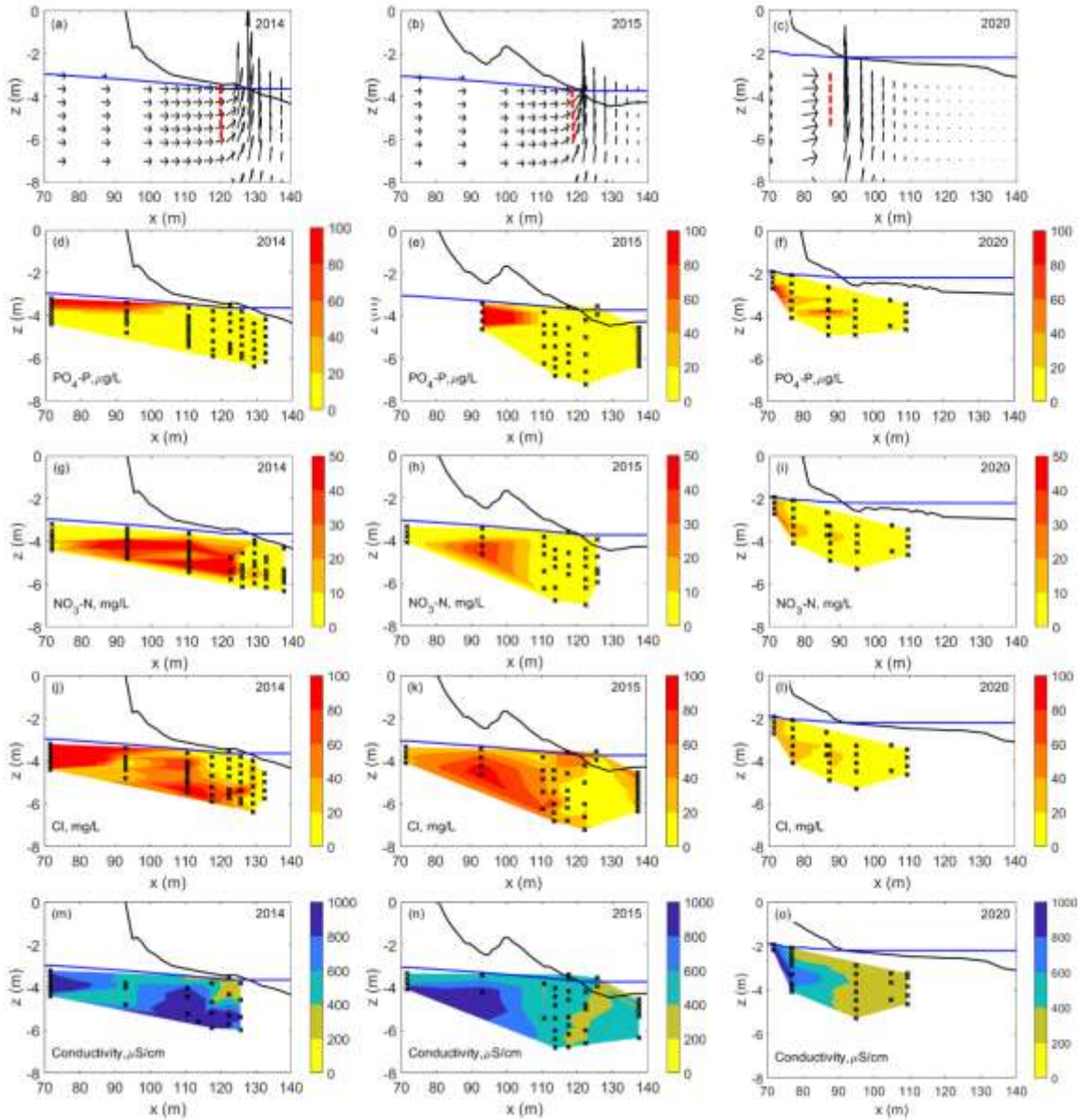


**Figure 4.** Simulated groundwater flow velocities based on the hydrological conditions during the a) 2014, b) 2015, and c) 2020 sampling periods. Distribution of d-f)  $\text{PO}_4\text{-P}$ , g-i)  $\text{NO}_3\text{-N}$ , j-l) chloride (Cl) and m-o) electrical conductivity (EC) in 2014, 2015 and 2020. For all subplots, the solid black line represents the sand surface elevation and the solid blue line represents the measured water levels for each sampling event. Red dashed lines in a-c) indicate lines across which  $\text{PO}_4\text{-P}$  and  $\text{NO}_3\text{-N}$  fluxes were calculated using the simulated groundwater fluxes and interpolated  $\text{PO}_4\text{-P}$  and  $\text{NO}_3\text{-N}$  concentrations ( $x = 120.3$  m in 2014 and 2015 and  $x = 88.7$  in 2020). Colored contours in d-o) represent the concentrations of  $\text{PO}_4\text{-P}$ ,  $\text{NO}_3\text{-N}$ , Cl and EC with the color bars shown on the right hand side, and black crosses show pore water sampling locations.

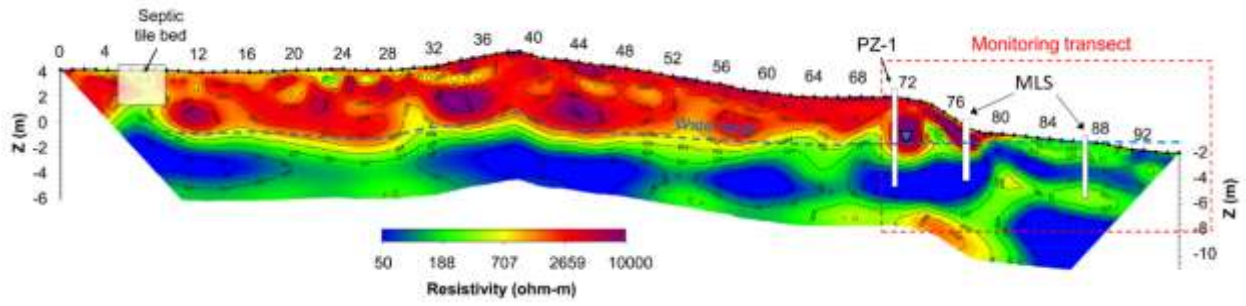


**Figure 5.** Cross-sectional resistivity image from the ERT survey. The septic drainage field, PZ-1 and MLS are indicated, along with the inferred water table (blue dashed line). The extent of the cross-shore monitoring transect is defined by the red dashed box.

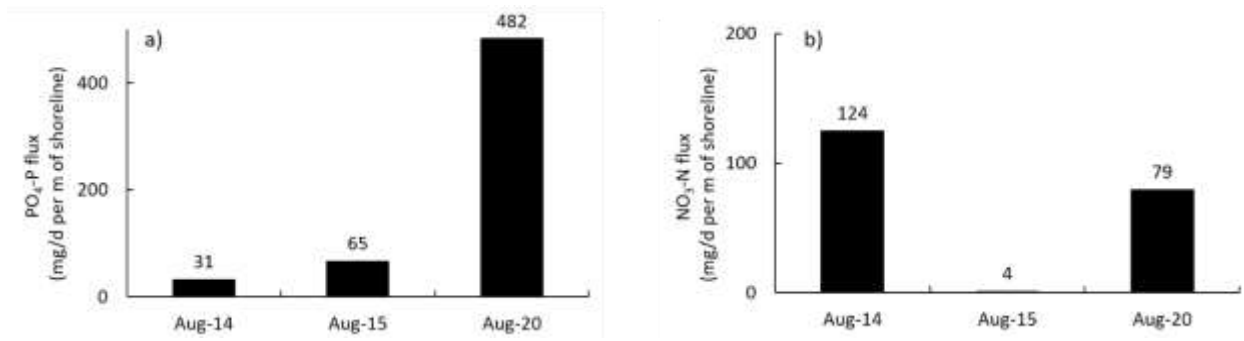


**Figure 6.** Estimated a)  $\text{PO}_4\text{-P}$  and b)  $\text{NO}_3\text{-N}$  flux directed towards the sediment-water interface for August 2014, 2015 and 2020 sampling events.

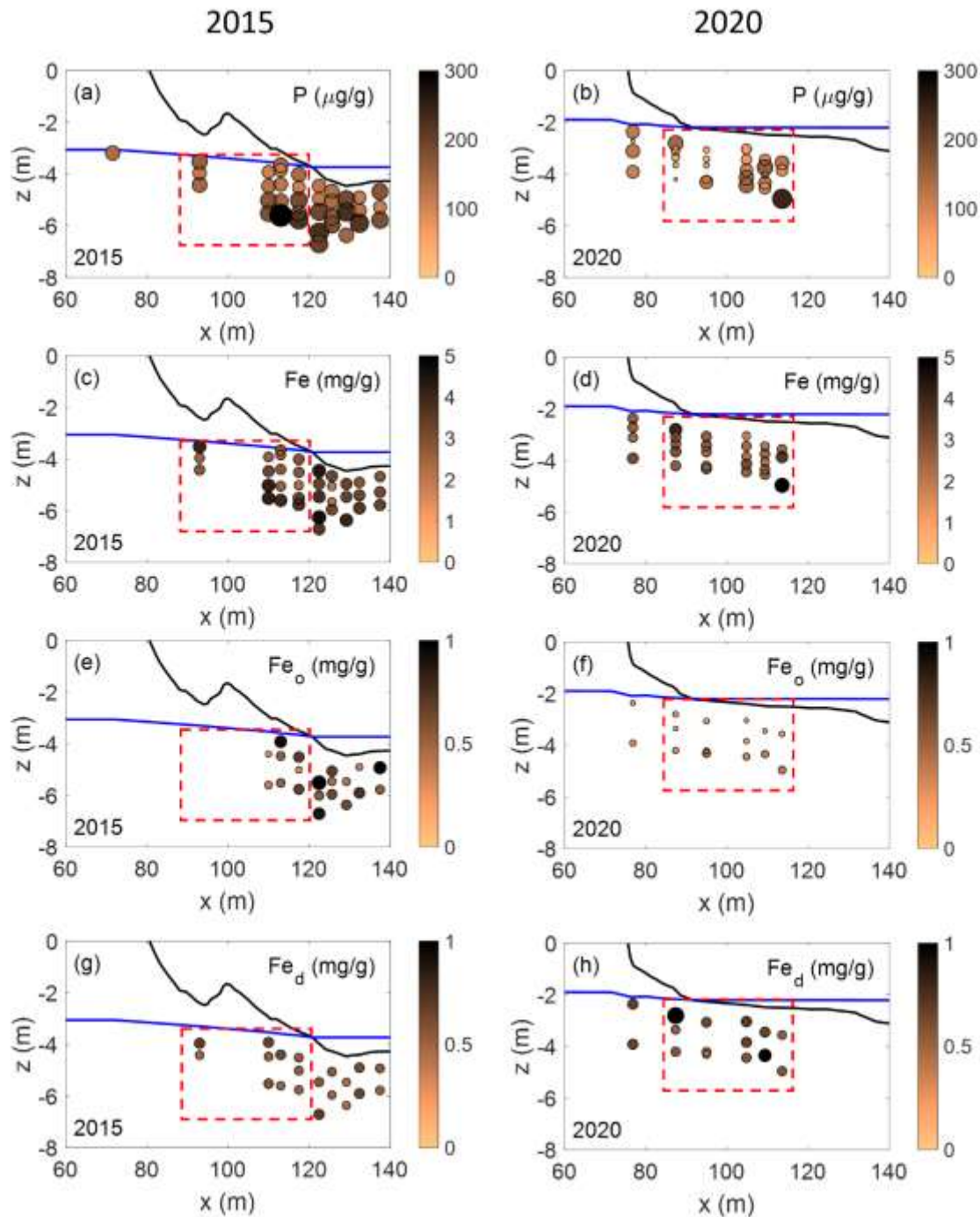


**Figure 7.** Distribution of a, e) solid-phase P, b, f) solid phase Fe, c, g) oxalate-extractable, amorphous Fe phases and d, h) dithionite-extractable, more crystalline Fe phases in 2015 and 2020. Rows show the year of sampling event when sediment sample was collected and columns show the different P and Fe solid phase extraction data. The bubble sizes and color bar indicate the magnitude of the solid-phase concentration. The solid black line represents the sand surface elevation, and the solid blue line represents the measured water levels at each site. Only the samples within the red box were considered in comparing the abundance of solid-phase P and Fe between sampling years.